Received: 26 March 2022 | Revised: 28 November 2022 | Accepted: 29 November 2022

DOI: 10.1111/ter.12638

REVIEW ARTICLE

Terra Nova WILEY

A Jurassic volcanic passive margin in Iran and Turkey

Hossein Azizi[1] | Robert J. Stern[2] | Raif Kandemir[3] | Orhan Karsli[4]

[1]Department of Mining, University of Kurdistan, Sanandaj, Iran

[2]Geosciences Department, University of Texas at Dallas, Richardson, Texas, USA

[3]Department of Geological Engineering, Recep Tayyip Erdoğan University, Rize, Turkey

[4]Department of Geological Engineering, Karadeniz Technical University, Trabzon, Turkey

Correspondence
Hossein Azizi, Department of Mining, University of Kurdistan, Sanandaj, Iran.
Email: azizi1345@gmail.com

Abstract

Broadly similar Early to Middle Jurassic stratigraphic sequences including bimodal igneous rocks of the Sanandaj–Sirjan Zone of Iran and the Sakarya Zone of Turkey suggest that these formed in a common tectonic setting in an extensional basin that evolved from a terrestrial magmatic rift to a marine shelf and passive continental margin. Whole-rock chemistry and Sr–Nd isotope signatures indicate derivation of mafic melts from partial melting of the subcontinental lithosphere. Decompression associated with extension led to 5%–30% partial melting of spinel–garnet lherzolite with minor involvement of continental crust, producing tholeiitic to transitional basaltic magma. Extensional basins inverted during the Mid-Late Jurassic. These relationships suggest the Early to Middle Jurassic formation of a volcanic rifted margin on the SW Eurasian margin, similar to that of offshore Norway.

1 | INTRODUCTION

At the centre of the Alpine-Himalaya orogenic belt, Iran and Turkey preserve similar evidence of different tectonic environments that have existed since the Ediacaran (Azizi & Whattam, 2022; Dokuz et al., 2022; Karsli et al., 2022; Moghadam et al., 2021). Magmatic activity in Turkey–Iran is limited to several intense episodes, including Ediacaran–Cambrian, late Palaeozoic, Jurassic, Late Cretaceous and Cenozoic (Azizi et al., 2019; Azizi & Tsuboi, 2021; Daneshvar et al., 2019; Gholipour et al., 2022; Karsli et al., 2022; Karsli, Dokuz, Faruk, & Bin, 2010; Karsli, Dokuz, Uysal, et al., 2010; Nouri et al., 2017; Nouri et al., 2021; Topuz et al., 2005; Topuz et al., 2017). Magmatic episodes reflected the opening and closing of Prototethys, Palaeotethys and Neotethys. The most enigmatic of these magmatic episodes happened in the Jurassic. Jurassic igneous rocks are not as well exposed as Cretaceous and Cenozoic magmatic rocks, which can be traced from western Iran to northern Turkey as parallel belts that formed at a convergent plate margin. Jurassic volcanic rocks in the central Sanandaj–Sirjan Zone (SaSZ) of Iran are interbedded with shallow marine sediments and intruded by granitic plutons. Based on clear OIB basaltic rocks with ages ~150 Ma in the central part of the SaSZ, bimodal magmatism and synsedimentary structures, a continental rift was suggested for the tectonic setting of the SaSZ in Jurassic time (Azizi et al., 2018; Azizi et al., 2020; Azizi & Stern, 2019).

In this contribution, we review Jurassic successions for Iran and northern Turkey as a "single terrane" hypothesis to test the hypothesis that these evolved as a continental rift. We show that Jurassic sequences in the two regions are usefully explained by the formation of a volcanic passive margin on the SW margin of Eurasia in Jurassic time. This novel interpretation further suggests that the Jurassic successions of Iran and Turkey offer an avenue for studying an exposed volcanic rifted margin as a complement to offshore studies (Gallahue et al., 2020).

1.1 | Jurassic rock sequences of Iran and Turkey

Jurassic rocks are widely distributed in northern, central and western Iran (Figure 1) and continue into the Sakarya Zone (SZ) of northern Turkey with minor exposures in southern and central Turkey (Ahadnejad et al., 2011; Azizi et al., 2011; Azizi, Najari, et al., 2015; Azizi, Zanjefili-Beiranvand, & Asahara, 2015; Bayati et al., 2017; Chiu et al., 2013; Çimen et al., 2018; Dokuz et al., 2017; Esna-Ashari et al., 2012; Eyuboglu et al., 2016; Fazlnia et al., 2009; Galoyan et al., 2018; Hunziker et al., 2015; Khalaji et al., 2007; Mahmoudi et al., 2011; Mousivand et al., 2011; Shahbazi et al., 2010; Stöcklin & Nabavi, 1973; Yilmaz & Bonhomme, 1991; Zhang et al., 2018). Jurassic sequences in Iran unconformably overlie Late Palaeozoic and Triassic rocks and start with terrestrial conglomerate, sandstone and shale, gradually changing up-section into marine limestone. These sediments are interbedded with mafic to felsic lavas and pyroclastics and are intruded by plutons and dikes. This succession attests to continental extension and subsidence in a terrestrial environment that evolved into a marine shelf. In the following, we describe the four main occurrences of Jurassic rocks in Iran and Turkey (Figure 1).

1.1.1 | Sanandaj–Sirjan Zone (SaSZ), Iran

The SaSZ Jurassic succession changed with time from older conglomerate, shale and sandstone into younger dolomite and limestone (Figure 2). Triassic sedimentary rocks (1000–1500 m thick) are unconformably overlain by Jurassic sedimentary rocks (700–3000 m thick). The Jurassic complex is overlain by Cretaceous shale and limestone which are interbedded with calc-alkaline basalts and andesites in the northern SaSZ.

1.1.2 | Central Iran

Jurassic sequences in central Iran are 200–1000 m thick and are preserved in NW–SE parallel basins (Figure 1). The Jurassic section in the Khur and Tabas regions (Figure 2) is similar to that of the SaSZ but sedimentation in the Tabas region continued from the Jurassic to Cretaceous (Figure 2).

1.1.3 | Northern Iran (Alborz)

In northern Iran, unconformities of the Jurassic section with the underlying Triassic and overlying Cretaceous sequences are clear (Figure 2). The main Jurassic unit is the ~4 km thick Shemshak formation of mainly siliciclastic rocks, terrigenous at the base and marine at the top (Fürsich et al., 2009).

1.1.4 | Northern Turkey, Sakarya Zone

Jurassic rocks in Turkey are mainly found in the eastern Sakarya Zone (SZ) and are more poorly developed elsewhere (Figure 1). These correlate with Iran Jurassic sequences, with similar discontinuities at the base and top. SZ sections (Akdoğan et al., 2019; Dokuz et al., 2017) also comprise sediments interbedded with basaltic rocks. Early–Middle Jurassic volcano-sedimentary rocks of the Şenköy Formation are widespread in the eastern SZ (Kandemir & Yilmaz, 2009) and rest unconformably on deformed Palaeozoic rocks. The Şenköy Formation varies from 2 to 2250 m thick, with significant vertical and lateral facies changes. An extensional tectonic environment is accepted for the deposition of these sequences (Kandemir & Yilmaz, 2009).

Dismembered Early Jurassic ophiolites with 186–174 Ma ages (Topuz, Çelik, et al., 2013; Topuz, Göçmengil, et al., 2013; Uysal, Akmaz, et al., 2015; Uysal, Ersoy, et al., 2015) are found in northern Turkey. These are around 20 Ma older than the sequences we discuss.

Significance Statement

What is Innovative

In this manuscript, we correlate Early to Middle Jurassic magmatism and sedimentation in Iran and Turkey and use this to propose an important new idea for the tectonic evolution of the region. We first show that rocks of the Sanandaj–Sirjan Zone and other Jurassic sequences in Iran have strong similarities to the Sakarya Zone in northern Turkey. We build on this result to show that the region at this time was affected by an extensional tectonic regime in a continental rift that evolved into a passive margin on the SW margin of Eurasia. Our work also shows how new advances in understanding the geology of this region can be obtained by Turkish and Iranian geoscientists working together.

What is of Broad General Interest

A complete reinterpretation of the Jurassic tectonic evolution of SW Eurasia will be of broad interest and is likely to be highly cited. This new interpretation is likely controversial, but we hope you agree that the idea deserves to be discussed.

2 | METHODS

We correlated Jurassic members units and compiled whole-rock chemical and Sr–Nd isotopic data for 216 Early to Middle Jurassic igneous rocks in Turkey, Armenia and Iran from the literature (Bozorg Seghinsara et al., 2017; Çimen, 2020; Doaee et al., 2020; Dokuz et al., 2010; Dokuz & Sünnetçi, 2019; Eyuboglu et al., 2016; Galoyan et al., 2018; Genç et al., 2010; Günay et al., 2019; Lechmann et al., 2018; Şen, 2007). We also compiled geochemical data for ophiolite mafic members with 184–176 Ma (Sarifakioğlu et al., 2009; Topuz, Göçmengil, et al., 2013; Uysal, Ersoy, et al., 2015); these are presented in Table S2 (whole rocks) and Table S3 (Sr–Nd isotopes). These data were used for identifying mafic rocks' tectonic settings. This information was used to develop a new geodynamic model for the Jurassic evolution of Turkey and Iran.

2.1 | Igneous Rock chemistry and Sr–Nd isotope ratios

Jurassic magmatism includes volcanic and intrusive rocks. Volcanic rocks are mainly basalt, andesite and rhyolite lava and tuff

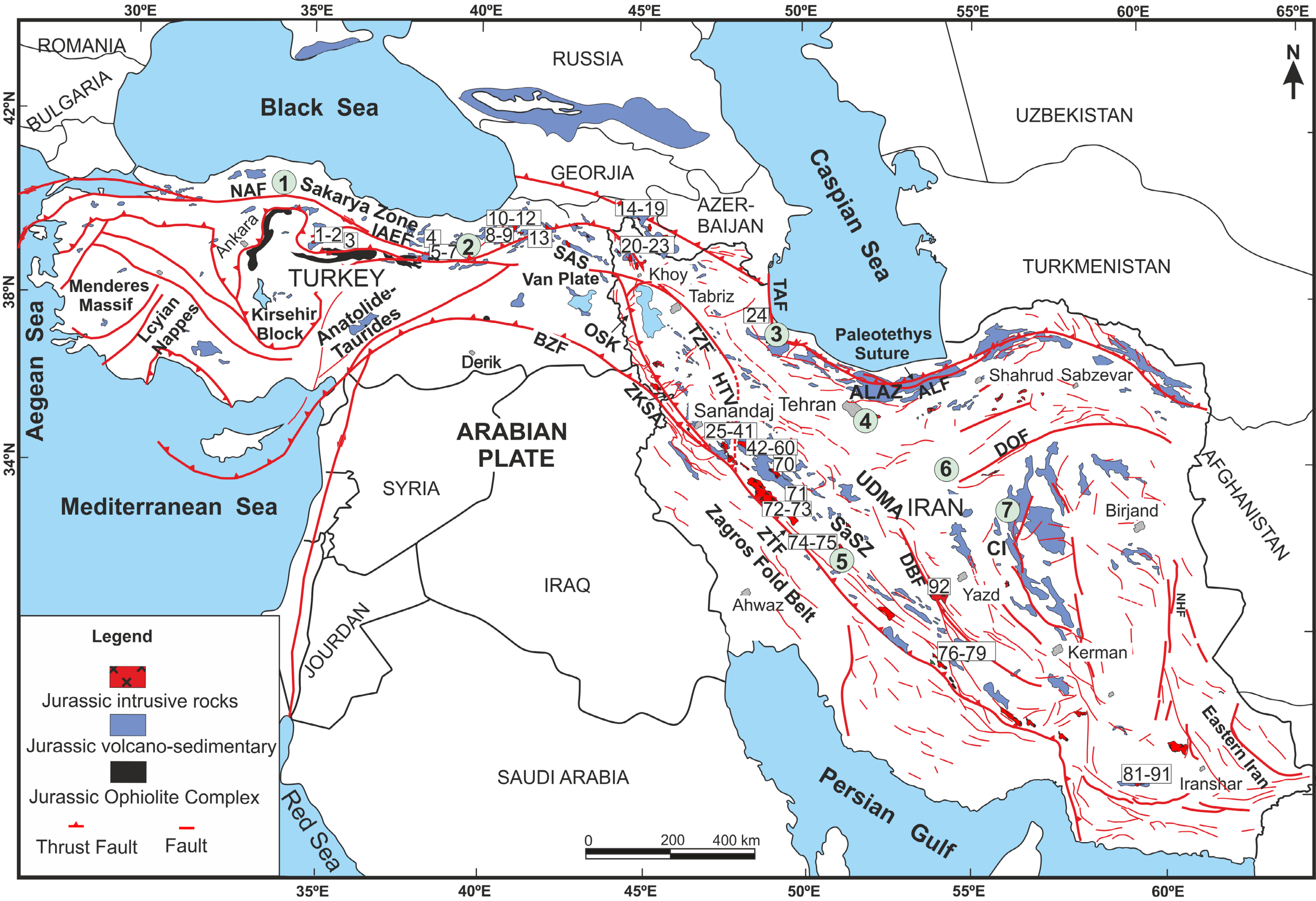

FIGURE 1 Distribution of Jurassic rocks in Turkey and Iran. Numbers in rectangles are ordered from west to east with ages by many researchers (Ahadnejad et al., 2011; Azizi et al., 2011; Azizi, Najari, et al., 2015; Azizi, Zanjefili-Beiranvand, & Asahara, 2015; Bayati et al., 2017; Chiu et al., 2013; Çimen et al., 2018; Deevsalar et al., 2017; Dokuz & Sünnetçi, 2019; Esna-Ashari et al., 2012; Eyuboglu et al., 2016; Fazlnia et al., 2007; Fazlnia et al., 2009; Galoyan et al., 2018; Hunziker et al., 2015; Khalaji et al., 2007; Lechmann et al., 2018; Madanipour et al., 2015; Mahmoudi et al., 2011; Shahbazi et al., 2010; Shakerardakani et al., 2015; Yilmaz & Bonhomme, 1991; Zhang et al., 2018). See Table S1 for more information. Pale green circles are stratigraphic column locations in Figure 2. ALAZ: Alborz–Azerbaijan Zone; ALF: Alborz Fault; BZF: Bitlis Zagros Fault; BZF: Bitlis–Zagros Fault; CI: Central Iran; DBF: Dehshir–Baft Fault; DOF: Dorouneh Fault; HTV: Hamadan–Tabriz Volcanic Belt; IAES: Izmir–Ankara–Erzincan Suture; NAF: Northern Anatolide Fault; NHF: Neh Fault; OSK: Oshnavieh–Salamas–Khoy Ophiolites; SAS: Sevan–Akera Suture; SaSZ: Sanandaj Sirjan Zone; TAF: Talesh Fault; TZF: Tabriz Fault; UDMA: Urumieh–Dokhtar Magmatic Ar; ZKSA: Zakros–Khoy–Sevan–Akera Suture. [Colour figure can be viewed at wileyonlinelibrary.com]

interbedded with sedimentary layers. Intrusive bodies vary from gabbro to granite. Chemical compositions in the Na_2O+K_2O versus SiO_2 (wt%) variation (Le Bas et al., 1986) are dominated by basaltic and acidic groups with subordinate intermediate rocks (Figure 3a). Mafic rocks mostly plot near the sub-alkaline and alkaline boundary with affinity to alkaline suites (Figure 3a). Due to the high $Fe_2O_3^t$ contents, most mafic rocks are tholeiites on the $Fe_2O_3^t$/MgO ratios versus SiO_2 diagram (Miyashiro, 1974) (Figure 3b). Mafic rocks also show a tholeiitic fractionation trend (Figure 3c) in the $Fe_2O_3^t$/MgO versus TiO_2 diagram (Miyashiro, 1973).

To avoid complications due to crustal contamination and magma differentiation for recognizing the tectonic setting of Jurassic magmatic rocks, we rely on samples with 45 to 52 wt% SiO_2 for interpretation Harker bivariant diagrams (Figure 4) with horizontal trends confirm that compositions change little as SiO_2 varies across this range, although minor variations suggest different magma sources. Mafic samples approach primary compositions and are useful for understanding the tectonic setting of formation. Mafic rocks with higher $Fe_2O_3^t$, TiO_2 and Y mainly plot in the tholeiitic field and extensional tectonic settings such as continental rift (Figure 5a–c) with minor arc affinities in some tectonic discrimination diagrams (Cabanis & Lecolle, 1989; Irvine & Baragar, 1971; Mullen, 1983). Higher Y with lower Zr contents (MacLean & Barrett, 1993) indicate tholeiitic and transitional basalts (Figure 6a). Some samples show arc affinity on the Nb/Th versus Nb diagram (Pearce, 2014) (Figure 6a). In the Ti–Vi variation diagram (Shervais, 1982), mafic rocks plot in the MORB to back-arc basin fields (Figure 6c). Due to elevated Ta/Hf and Th/Hf ratios (Figure 6d), samples mostly plot in the rift initiation to mature continental rift and some in the mantle plume field (Yunliang et al., 2001). Lower Th/Yb and higher Nb/Yb ratios (Pearce, 2008) show the relation of these rocks to normal mid-oceanic ridge basalt (N-MORB) and oceanic island basalt (OIB)

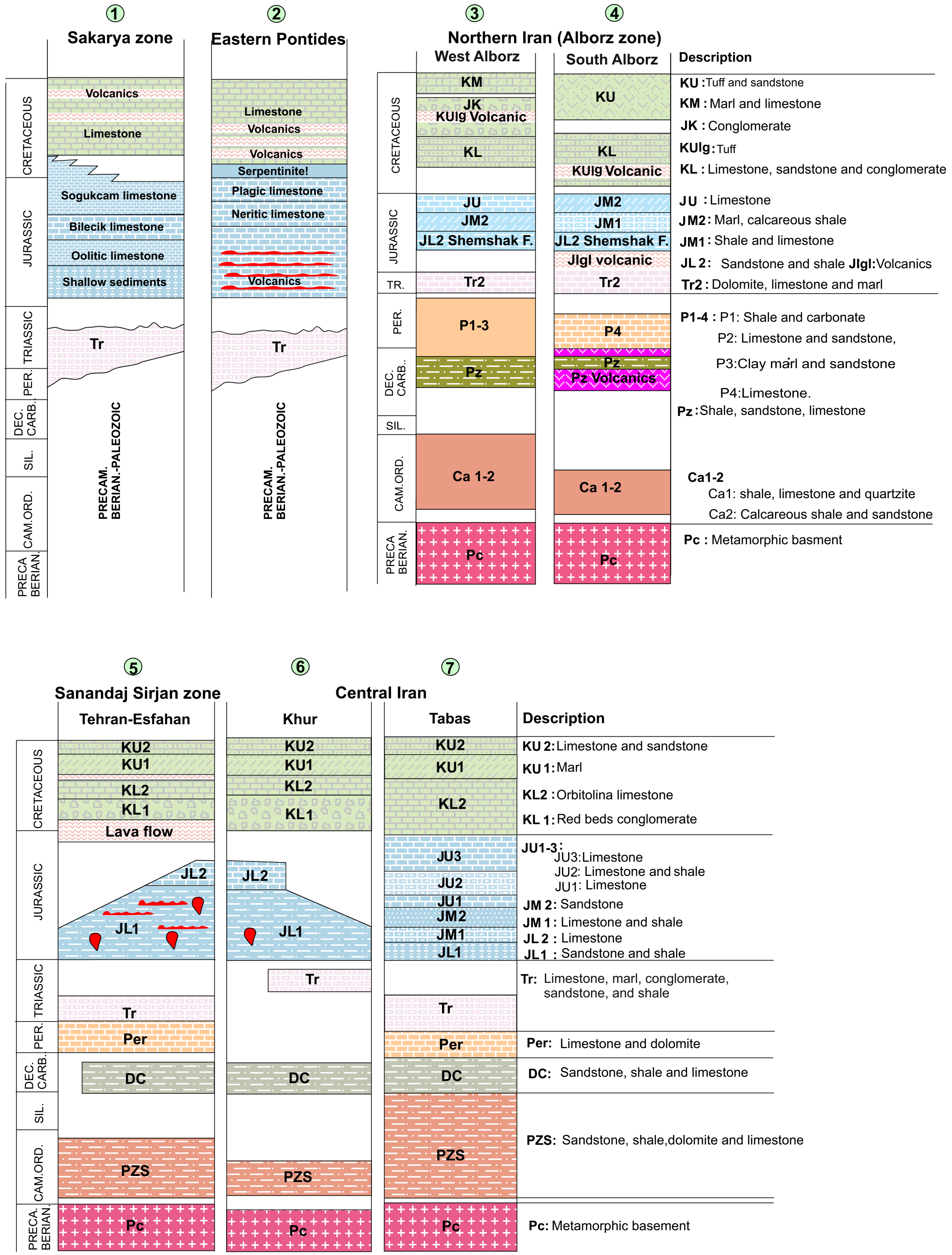

FIGURE 2 Simplified stratigraphic columns of Turkey (1 and 2) and Iran (3–7). Columns 1 and 2 are modified from (Akdoğan et al., 2019; Dokuz et al., 2017). Columns 3–7 are modified from the geological map of Iran (Huber, 1977). See the location of stratigraphical columns in Figure 1. [Colour figure can be viewed at wileyonlinelibrary.com]

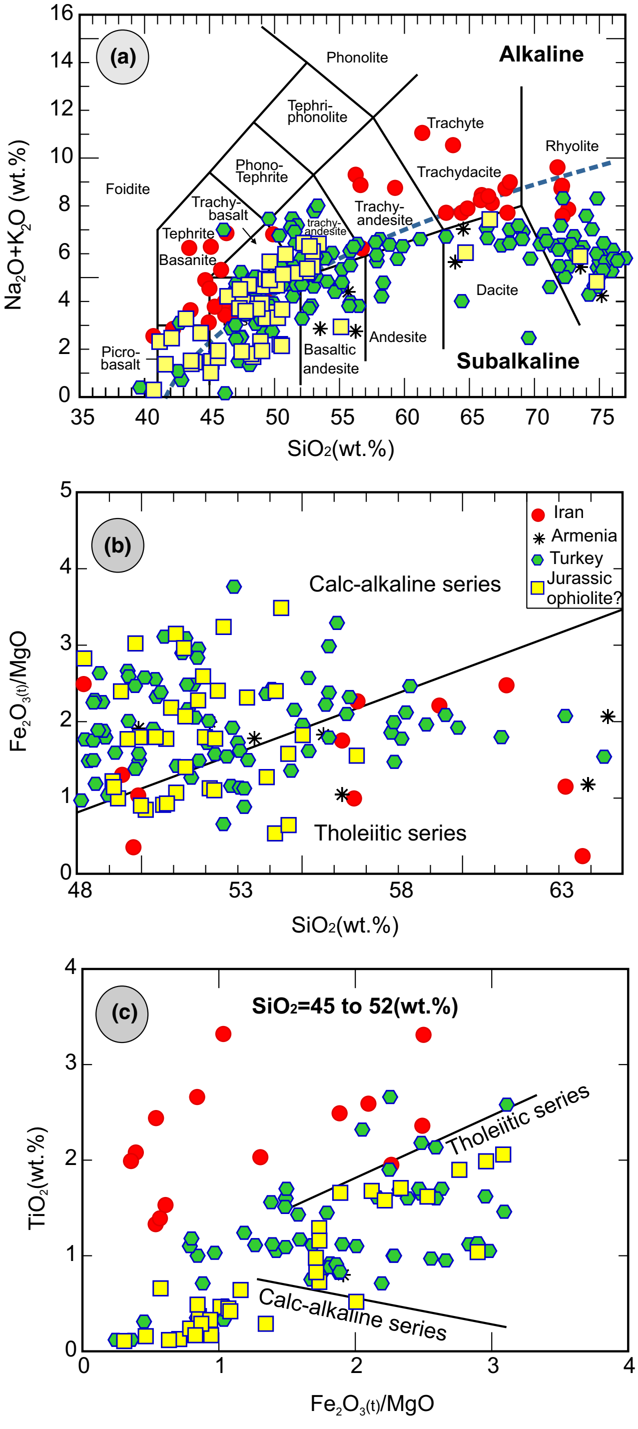

FIGURE 3 Chemistry of Jurassic volcanic and intrusive rocks (Bozorg Seghinsara et al., 2017; Çimen, 2020; Doaee et al., 2020; Dokuz et al., 2010; Dokuz & Sünnetçi, 2019; Eyuboglu et al., 2016; Galoyan et al., 2018; Genç et al., 2010; Günay et al., 2019; Lechmann et al., 2018; Şen, 2007) and mafic parts of the Early Jurassic ophiolites (Sarifakioğlu et al., 2009; Topuz, Göçmengil, et al., 2013; Uysal, Ersoy, et al., 2015). Chemical compositions range from mafic to felsic in the Na_2O+K_2O versus SiO_2 (Le Bas et al., 1986) and are dominated by basaltic and acidic groups with subordinate intermediate rocks (a). (b and c) Fe_2O_3(t)/MgO versus SiO_2 and TiO_2 diagrams (Miyashiro, 1974). [Colour figure can be viewed at wileyonlinelibrary.com]

with minor crustal assimilation (Figure 6e). Minor continental crustal contamination (Figure 6f) is also seen on plots of Nb/La versus Nb/Th ratios (Zhang et al., 2014).

Low La/Yb and high La/Sm ratios and high Sm concentrations in mafic rocks show that these magmas were produced from the partial melting of mostly spinel–garnet peridotites and minor garnet lherzolite (Figure 6g–i). Modelled partial melting of the spinel–garnet lherzolite (Aldanmaz et al., 2000) shows these were generated from 5 to 30% partial melting.

The samples mostly have low to moderate $^{87}Sr/^{86}Sr(t)$ (from 0.7036 to 0.7087, mean = 0.7052), moderate $\varepsilon_{Nd}(t)$ (+6 to −2, mean = +2.8, n = 67; Figure 7) and Nd model ages (T_{DM} = 0.32 to 1.4 Ga, mean = 0.78 Ga) (Table S3). These rocks mostly plot in the depleted mantle field. Scatter in the $^{87}Sr/^{86}Sr(t)$ versus $\varepsilon_{Nd}(t)$ diagram suggests that some samples were affected by seawater alteration, but this could also indicate the involvement of old subduction-modified crust or lithosphere.

3 | DISCUSSION

Due to the time progression of Jurassic intrusions in the central SaSZ and bimodal magmatism, a propagating continental rift was suggested for the C-SaSZ (Azizi & Stern, 2019). In this discussion, we build on this insight to show that the SaSZ and correlative Jurassic sequences in northern Turkey and Iran were parts of a volcanic passive margin that began to form during the Jurassic. This interpretation is supported by the presence of basaltic rocks with a plume to N-MORB type affinities.

Jurassic basaltic rocks interbedded with sediments are also abundant in northern and central Iran. If we accept the increasingly convincing evidence that Neotethys subduction beneath Iran began in mid-Cretaceous time (Azizi & Stern, 2019; Balázs et al., 2021; Gholipour et al., 2021; Moghadam & Stern, 2021; Stern et al., 2021), an interpretation that is supported by the development of ~100 Ma high-*P* metamorphism (Angiboust et al., 2016), we can entertain two possibilities for the evolution of Jurassic marine sedimentation and magmatism in Iran and Turkey.

The first scenario emphasizes the development of a Jurassic basin system with the basal conglomerate and older sedimentary layers accompanied by bimodal magmatism. Basaltic magmas were generated from the partial melting of spinel to garnet lherzolite of the subcontinental lithospheric mantle. The different types of sediments with similar ages and the absence of Jurassic sediments in some areas suggest that Jurassic basins opened in central, north and southern Iran as well as in northern Turkey. Such distributed extension is common in the early stages of continental breakup, for example, in the Triassic of the eastern USA (Withjack et al., 2020). From this perspective, Jurassic basins may have accompanied the opening of Neotethys. This interpretation finds further support because younger Jurassic and Early Cretaceous deep marine sediments such

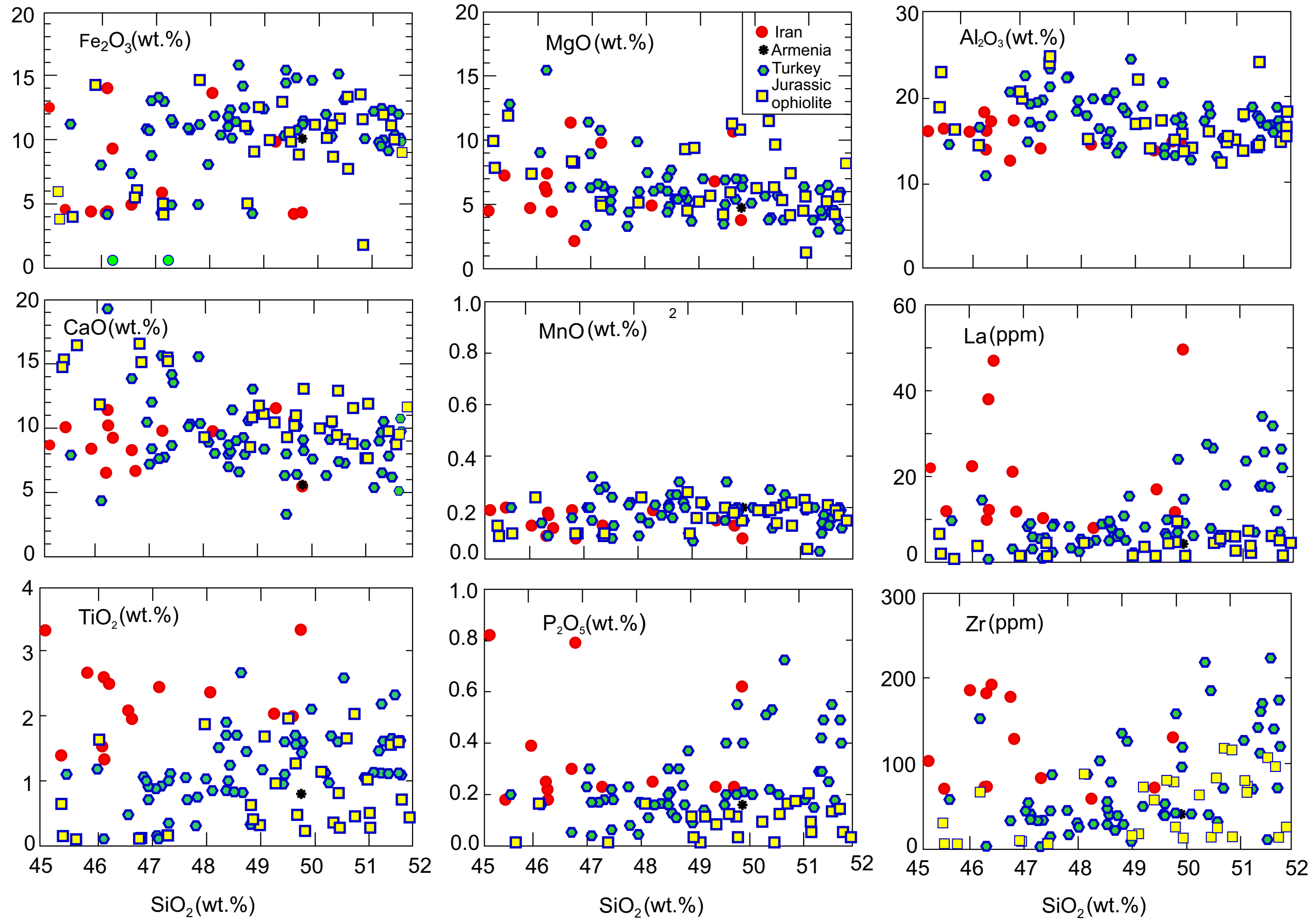

FIGURE 4 Harker bivariant diagrams for Jurassic mafic samples (Bozorg Seghinsara et al., 2017; Çimen, 2020; Doaee et al., 2020; Dokuz et al., 2010; Dokuz & Sünnetçi, 2019; Eyuboglu et al., 2016; Galoyan et al., 2018; Genç et al., 2010; Günay et al., 2019; Lechmann et al., 2018; Şen, 2007) and mafic parts of the Early Jurassic ophiolites (Sarifakioğlu et al., 2009; Topuz, Göçmengil, et al., 2013; Uysal, Ersoy, et al., 2015) with SiO_2 contents between 45 and 52 wt%. [Colour figure can be viewed at wileyonlinelibrary.com]

as chert and radiolarites are exposed throughout Zagros, demonstrating subsidence to pelagic depths (Al-Qayim et al., 2018).

Jurassic basins in Iran and Turkey were inverted and exposed during the Late Jurassic–Early Cretaceous. These rocks were eroded and covered by the middle Cretaceous basal conglomerate. Based on these findings we suggest an integrated model for the Jurassic–Cretaceous evolution of SW Eurasia with three main elements: (a) Jurassic continental rifting with bimodal magmatism to open a wide extensional basin system along and adjacent to the continental crust margin; (b) thermal subsidence to form a Late Jurassic–Earliest Cretaceous passive continental margin on the northern flank of Neotethys; and (c) subduction initiation of Neotethys beneath Iran–Turkey in the mid-Cretaceous. This model is presented in Figure 8a–c.

The second scenario involves the southward subduction of Palaeotethys. Palaeotethys is generally accepted to have formed in Permo-Triassic time on the north side of Iran and Turkey. Some researchers accept that Palaeotethys subducted northward beneath Eurasia (Alavi, 1991; Zanchi et al., 2009; Karimpour et al., 2010; Hassanpour, 2021; Okay and Şahintürk, 1997). Others consider southward subduction of Palaeotethys beneath northern Turkey continued into Jurassic time to form a back-arc basin in the Sakarya Zone (Dokuz et al., 2010; Genç et al., 2010; Kandemir & Yilmaz, 2009; Karsli et al., 2017; Maffione & van Hinsbergen, 2018; Sengör & Yilmaz, 1981). This interpretation is precluded for Iran, where Palaeotethys closed in Permo-Triassic time (Moghadam and Stern, 2014). For this reason, we prefer the continental rift-passive margin scenario.

4 | CONCLUSIONS

Jurassic extensional basins developed in Iran and Turkey during Early–Middle Jurassic time, associated with bimodal magmatism. Chemical compositions and Sr–Nd isotope ratios suggest the derivation of mafic melts from the partial melting of spinel–garnet lherzolite. 5%–30% partial melting in an extensional tectonic regime with minor involvement of continental crust is suggested for the sources of tholeiitic to alkalic basaltic magma. We suggest two main scenarios for the SW Eurasian Jurassic extensional regime

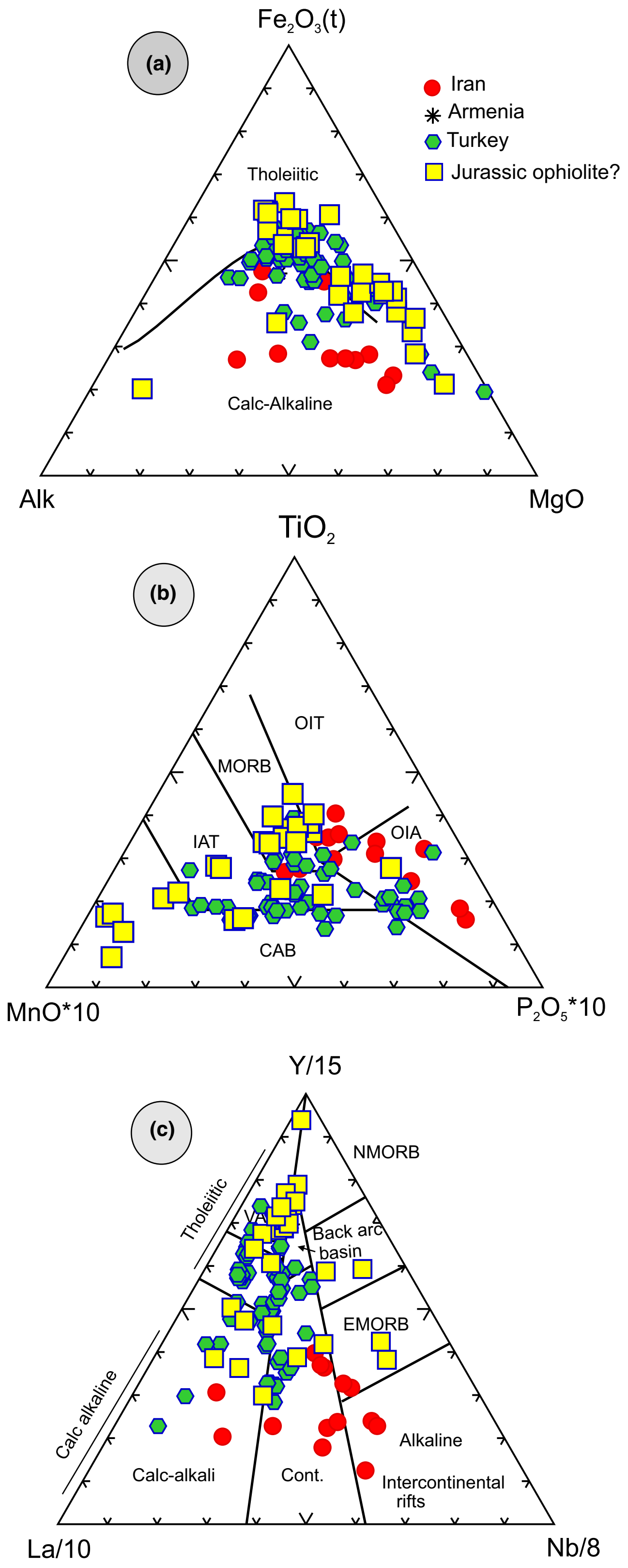

FIGURE 5 Mafic samples with higher contents of Fe_2O_3(t), TiO_2 and Y (Bozorg Seghinsara et al., 2017; Çimen, 2020; Doaee et al., 2020; Dokuz et al., 2010; Dokuz & Sünnetçi, 2019; Eyuboglu et al., 2016; Galoyan et al., 2018; Genç et al., 2010; Günay et al., 2019; Lechmann et al., 2018; Şen, 2007) and mafic parts of the Early Jurassic ophiolite (Sarifakioğlu et al., 2009; Topuz, Göçmengil, et al., 2013; Uysal, Ersoy, et al., 2015) (a and b) mainly plot in the tholeiitic and calc-alkaline field (Irvine & Baragar, 1971) Island arc, MORB and oceanic island basalts (Mullen, 1983) and (c) extensional tectonic regimes such as continental rift (Cabanis & Lecolle, 1989). [Colour figure can be viewed at wileyonlinelibrary.com]

which differ mainly concerning whether Turkey–Iran was part of Eurasia (Palaeotethys closed) or not (Palaeotethys open). Evidence from NE Iran that Palaeotethys closed thereby Early Triassic time and closed later north of Turkey indicates that Jurassic extensional basins are not related to Palaeotethys subduction. Turkey–Iran extensional basins experienced intense magmatic and tectonic activity in the Mid-Late Jurassic and inverted in the Early Cretaceous. These relationships suggest the formation of a Jurassic-rifted continental margin on the SW margin of Eurasia. Further work is needed to test the hypothesis of the Jurassic formation of a volcanic-rifted passive margin on the SW Eurasian margin, similar to that of offshore Norway, but the advantages of Iranian and Turkish scientists working together to solve common geoscientific problems are clear.

ACKNOWLEDGEMENTS

F. Nouri and N. Daneshvar helped to generate two figures. This work benefited from two reviewers, an anonymous associate editor, and a scientific editor K. Mezger. This is UTD Geosciences contribution #1698.

DATA AVAILABILITY STATEMENT

The data that supports the findings of this study are available in the supplementary material of this article.

ORCID

Hossein Azizi https://orcid.org/0000-0001-5686-4340
Robert J. Stern https://orcid.org/0000-0002-8083-4632

REFERENCES

Ahadnejad, V., Valizadeh, M. V., Deevsalar, R., & Rezaei-Kahkhaei, M. (2011). Age and geotectonic position of the Malayer granitoids: Implication for plutonism in the Sanandaj-Sirjan Zone, W Iran. *Neues Jahrbuch für Geologie und Paläontologie - Abhandlungen*, *261*, 61–75. https://doi.org/10.1127/0077-7749/2011/0149

Akdoğan, R., Okay, A. I., & Dunkl, I. (2019). Striking variation in the provenance of the Lower and Upper Cretaceous turbidites in the Central Pontides (Northern Turkey) related to the opening of the Black Sea. *Tectonics*, *38*, 1050–1069.

Alavi, M. (1991). Sedimentary and structural characteristics of the Paleo-Tethys remnants in Northeastern Iran. *Geological Society of America Bulletin*, *103*, 983. https://doi.org/10.1130/0016-7606(1991)103<0983:SASCOT>2.3.CO;2

Aldanmaz, E., Pearce, J. A., Thirlwall, M. F., & Mitchell, J. G. (2000). Petrogenetic evolution of late Cenozoic, post-collision volcanism in western Anatolia, Turkey. *Journal of Volcanology and Geothermal Research*, *102*, 67–95. https://doi.org/10.1016/S0377-0273(00)00182-7

Al-Qayim, B. A., Baziany, M. M., & Ameen, B. M. (2018). Mesozoic tethyan radiolarite age determination, zagros suture zone, Kurdistan, Ne Iraq. *Iraqi Geological Journal*, *51*, 17–33.

Angiboust, S., Agard, P., Glodny, J., Omrani, J., & Oncken, O. (2016). Zagros blueschists: Episodic underplating and long-lived cooling of

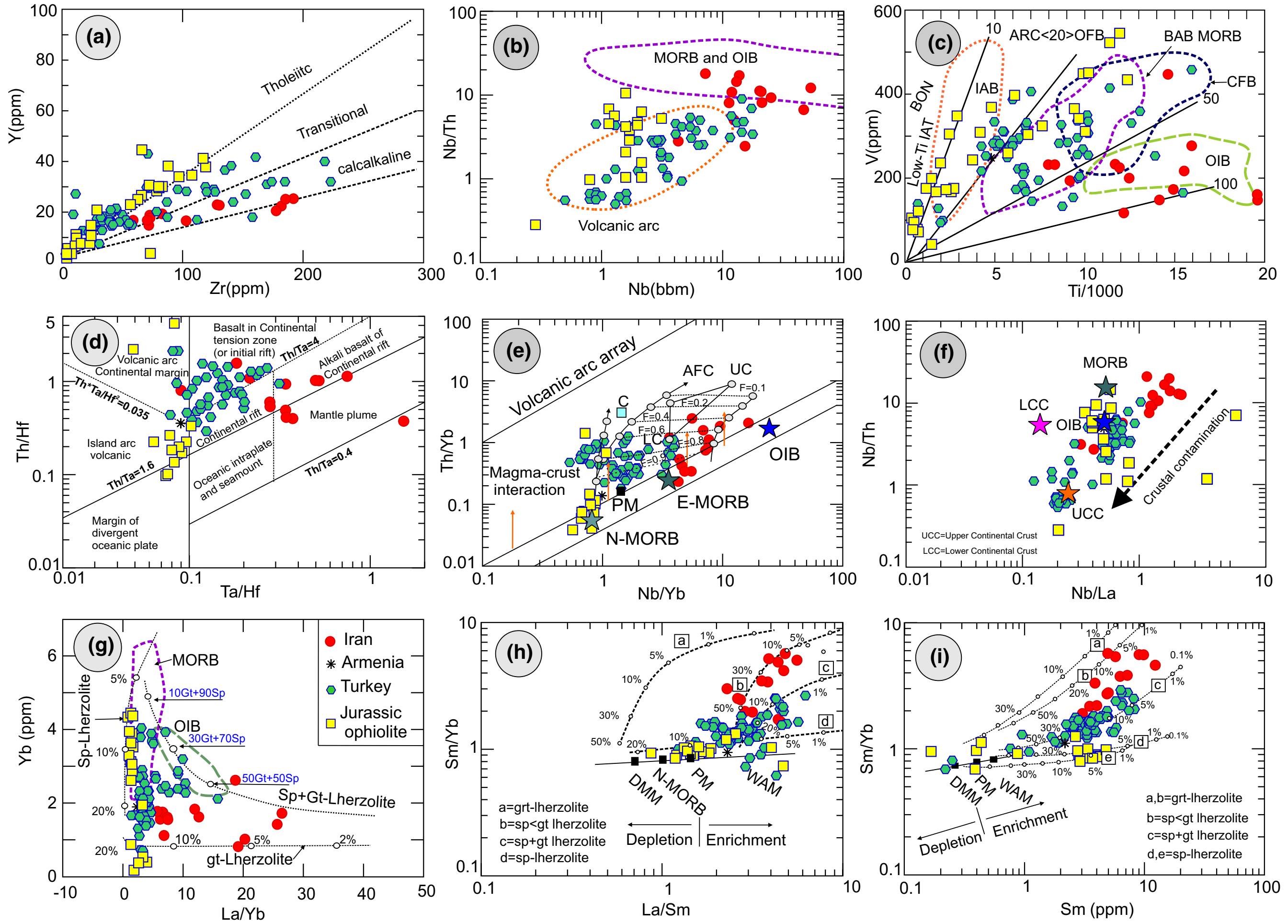

FIGURE 6 Mafic samples (Bozorg Seghinsara et al., 2017; Çimen, 2020; Doaee et al., 2020; Dokuz et al., 2010; Dokuz & Sünnetçi, 2019; Eyuboglu et al., 2016; Galoyan et al., 2018; Genç et al., 2010; Günay et al., 2019; Lechmann et al., 2018; Şen, 2007) and mafic parts of the Early Jurassic ophiolite (Sarifakioğlu et al., 2009; Topuz, Göçmengil, et al., 2013; Uysal, Ersoy, et al., 2015) in some petrogenetic variation diagrams (a) Zr versus Y contents (MacLean & Barrett, 1993), (b) Nb/Th versus Nb (Pearce, 2014), (c) Ti-Vi (Shervais, 1982), (d) Ta/Hf versus Th/Hf ratios (Yunliang et al., 2001), (e) Th/Yb versus Nb/Yb ratios (Pearce, 2008), (f) Nb/La versus Nb/Th ratios in some areas (Zhang et al., 2014) show the relation of these rocks to normal mid-oceanic ridge basalt (N-MORB) and oceanic island basalt (OIB) with minor crustal assimilation. (g–i) Yb versus La/Yb and La/Sm and also Sm versus Sm/Yb ratios (Aldanmaz et al., 2000) consistent with the interpretation that these magmas were produced from partial melting of spinel–garnet peridotite and minor garnet lherzolite. See the text for more information. [Colour figure can be viewed at wileyonlinelibrary.com]

a subduction zone. *Earth and Planetary Science Letters*, *443*, 48–58. https://doi.org/10.1016/j.epsl.2016.03.017

Azizi, H., & Asahara, Y. (2013). Juvenile granite in the Sanandaj-Sirjan Zone, NW Iran: Late Jurassic-Early Cretaceous arc-continent collision. *International Geology Review*, *55*, 1523–1540. https://doi.org/10.1080/00206814.2013.782959

Azizi, H., Asahara, Y., Mehrabi, B., & Chung, S. L. (2011). Geochronological and geochemical constraints on the petrogenesis of high-K granite from the Suffi abad area, Sanandaj-Sirjan Zone, NW Iran. *Chemie der Erde Geochemistry*, *71*, 363–376. https://doi.org/10.1016/j.chemer.2011.06.005

Azizi, H., Lucci, F., Stern, R. J. R. J., Hasannejad, S., & Asahara, Y. (2018). The Late Jurassic Panjeh submarine volcano in the northern Sanandaj-Sirjan Zone, northwest Iran: Mantle plume or active margin? *Lithos*, *308–309*, 364–380. https://doi.org/10.1016/j.lithos.2018.03.019

Azizi, H., Najari, M., Asahara, Y., Catlos, E. J., Shimizu, M., & Yamamoto, K. (2015). U-Pb zircon ages and geochemistry of Kangareh and Taghiabad mafic bodies in northern Sanandaj-Sirjan Zone, Iran: Evidence for intra-oceanic arc and back-arc tectonic regime in Late Jurassic. *Tectonophysics*, *660*, 47–64. https://doi.org/10.1016/j.tecto.2015.08.008

Azizi, H., Nouri, F., Stern, R. J. R. J., Azizi, M., Lucci, F., Asahara, Y., Zarinkoub, M. H., & Chung, S. L. S. L. S. L. (2020). New evidence for Jurassic continental rifting in the northern Sanandaj Sirjan Zone, western Iran: the Ghalaylan seamount, southwest Ghorveh. *International Geology Review*, *62*, 1635–1657. https://doi.org/10.1080/00206814.2018.1535913

Azizi, H., & Stern, R. J. (2019). Jurassic igneous rocks of the central Sanandaj–Sirjan zone (Iran) mark a propagating continental rift, not a magmatic arc. *Terra Nova*, *31*, 415–423. https://doi.org/10.1111/ter.12404

Azizi, H., Stern, R. J., Topuz, G., Asahara, Y., & Shafaii Moghadam, H. (2019). Late Paleocene adakitic granitoid from NW Iran and comparison with adakites in the NE Turkey: Adakitic melt generation in normal continental crust. *Lithos*, *346–347*, 105151. https://doi.org/10.1016/J.Lithos.2019.105151

Azizi, H., & Tsuboi, M. (2021). The van microplate: A new microcontinent at the junction of Iran, Turkey, and Armenia. *Frontiers in Earth Science*, *8*, 574385. https://doi.org/10.3389/feart.2020.574385

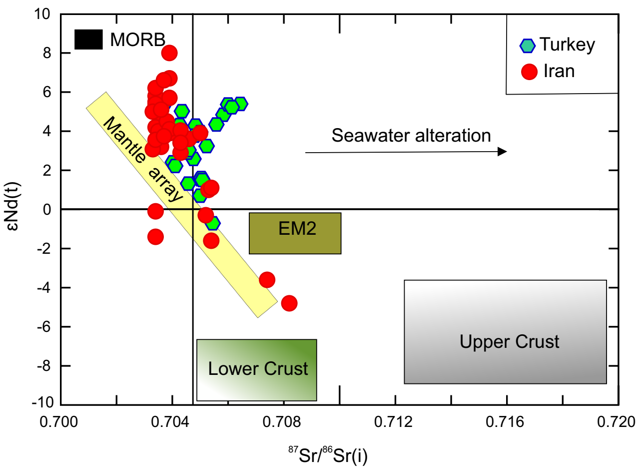

FIGURE 7 Initial $^{87}Sr/^{86}Sr$ ratios and εNd(t) for Jurassic mafic igneous rocks from Turkey (Dokuz et al., 2010; Dokuz & Sünnetçi, 2019; Eyuboglu et al., 2016; Genç & Tüysüz, 2010; Lechmann et al., 2018; Şen, 2007) and the SaSZ of Iran (Ahadnejad et al., 2011; Azizi et al., 2011; Azizi & Asahara, 2013; Azizi, Najari, et al., 2015; Azizi & Stern, 2019; Deevsalar et al., 2017), calculated for t = 170–150 Ma. These rocks mostly plot in the depleted mantle field with minor evidence for crustal contamination and/or seawater alteration. See text for further explanation. References and data are listed in Table S3. [Colour figure can be viewed at wileyonlinelibrary.com]

Azizi, H., & Whattam, S. A. (2022). Does neoproterozoic-early paleozoic (570–530 Ma) basement of Iran belong to the cadomian orogeny? *Precambrian Research*, *368*, 106474. https://doi.org/10.1016/J.PRECAMRES.2021.106474

Azizi, H., Zanjefili-Beiranvand, M., & Asahara, Y. (2015). Zircon U–Pb ages and petrogenesis of a tonalite–trondhjemite–granodiorite (TTG) complex in the northern Sanandaj–Sirjan zone, northwest Iran: Evidence for Late Jurassic arc–continent collision. *Lithos*, *216*, 178–195. https://doi.org/10.1016/j.lithos.2014.11.012

Balázs, A., Faccenna, C., Ueda, K., Funiciello, F., Boutoux, A., Blanc, E. J.-P., & Gerya, T. (2021). Oblique subduction and mantle flow control on upper plate deformation: 3D geodynamic modeling. *Earth and Planetary Science Letters*, *569*, 117056. https://doi.org/10.1016/j.epsl.2021.117056

Bayati, M., Esmaeily, D., Maghdour-Mashhour, R., Li, X. H., & Stern, R. J. (2017). Geochemistry and petrogenesis of Kolah-Ghazi granitoids of Iran: Insights into the Jurassic Sanandaj-Sirjan magmatic arc. *Chemie der Erde - Geochemistry*, *77*, 281–302. https://doi.org/10.1016/j.chemer.2017.02.003

Bozorg Seghinsara, R., Sheikhi Karizaki, H., Moazzen, M., Pourkermani, M., & Ashja Ardalan, A. (2017). Whole rock geochemistry and tectonic setting of jurassic aged Lisar Granite, Talesh Mountains, North Iran: Bulletin of the Mineral. *Research and Exploration*, *2017*, 99–113. https://doi.org/10.19111/bulletinofmre.336499

Cabanis, B., & Lecolle, M. (1989). Le diagramme La/10–Y/15–Nb/8: un outil pour la discrimination des séries volcaniques et la mise en évidence des processus de melange et/ou de contamination crustale. *Mécanique, physique, chimie, sciences de l'univers, sciences de Comptes rendus de l'Académie des Sciences*, *II*, 2023–2029.

Chiu, H. Y., Chung, S. L., Zarrinkoub, M. H., Mohammadi, S. S., Khatib, M. M., & Iizuka, Y. (2013). Zircon U-Pb age constraints from Iran on the magmatic evolution related to Neotethyan subduction and Zagros orogeny. *Lithos*, *162–163*, 70–87. https://doi.org/10.1016/j.lithos.2013.01.006

Çimen, O. (2020). Geochemical characteristics of a pre-Middle Jurassic oceanic crust fragment from the Central Pontides in northern Turkey: Geodynamic implications on intra-oceanic subduction initiation. *Chemie der Erde*, *80*, 125535. https://doi.org/10.1016/j.chemer.2019.125535

Çimen, O., Göncüoğlu, M. C., Simonetti, A., & Sayit, K. (2018). New zircon U-Pb LA-ICP-MS ages and Hf isotope data from the Central Pontides (Turkey): Geological and geodynamic constraints. *Journal of Geodynamics*, *116*, 23–36. https://doi.org/10.1016/j.jog.2018.01.004

Daneshvar, N., Maanijou, M., Azizi, H., & Asahara, Y. (2019). Petrogenesis and geodynamic implications of an Ediacaran (550 Ma) granite complex (metagranites), southwestern Saqqez, northwest Iran. *Journal of Geodynamics*, *132*, 101669. https://doi.org/10.1016/j.jog.2019.101669

Deevsalar, R., Shinjo, R., Ghaderi, M., Murata, M., Hoskin, P. W. O., Oshiro, S., Wang, K. L., Lee, H. Y., & Neill, I. (2017). Mesozoic–Cenozoic mafic magmatism in Sanandaj–Sirjan Zone, Zagros Orogen (Western Iran): Geochemical and isotopic inferences from Middle Jurassic and Late Eocene gabbros. *Lithos*, *284–285*, 588–607. https://doi.org/10.1016/J.lithos.2017.05.009

Doaee, A. K., Ghorbani, G., & Sadeghian, M. (2020). Geochemistry and petrology of gabbrodiorites from Palang Dar Area (Northeast Damghan). *Iranian Journal of Crystallography and Mineralogy*, *28*, 751–762. https://doi.org/10.29252/ijcm.28.3.751

Dokuz, A., Aydınçakır, E., Kandemir, R., Karslı, O., Siebel, W., Derman, A. S., & Turan, M. (2017). Late Jurassic magmatism and stratigraphy in the Eastern Sakarya zone, Turkey: Evidence for the slab breakoff of paleotethyan oceanic lithosphere. *Journal of Geology*, *125*, 1–31. https://doi.org/10.1086/689552

Dokuz, A., Gucer, M. A., Krasli, O., & Keewook, Y. (2022). From Cadominan Back-arc basin to Rheic Ocean closure: The geochronological records of the Kurtoglu massif, eastern Sakrya Zone, Turkey. *International Journal of Earth Science*, *111*, 1333–1355.

Dokuz, A., Karsli, O., Chen, B., & Uysal, I. (2010). Sources and petrogenesis of Jurassic granitoids in the Yusufeli area, Northeastern Turkey: Implications for pre- and post-collisional lithospheric thinning of the eastern Pontides. *Tectonophysics*, *480*, 259–279. https://doi.org/10.1016/j.tecto.2009.10.009

Dokuz, A., & Sünnetçi, K. (2019). Jurassic acidic magmatism in a back-arc setting, eastern Sakarya Zone, Turkey: Geochemical constraints and an evolutionary model. *Lithos*, *332–333*, 312–327. https://doi.org/10.1016/j.lithos.2019.02.022

Esna-Ashari, A., Tiepolo, M., Valizadeh, M.-V. V., Hassanzadeh, J., & Sepahi, A.-A. A. (2012). Geochemistry and zircon U-Pb geochronology of Aligoodarz granitoid complex, Sanandaj-Sirjan Zone, Iran. *Journal of Asian Earth Sciences*, *43*, 11–22. https://doi.org/10.1016/j.jseaes.2011.09.001

Eyuboglu, Y., Dudas, F. O., Santosh, M., Xiao, Y., Yi, K., Chatterjee, N., Wu, F. Y., & Bektaş, O. (2016). Where are the remnants of a Jurassic Ocean in the eastern Mediterranean region? *Gondwana Research*, *33*, 63–91. https://doi.org/10.1016/j.gr.2015.08.017

Fazlnia, A., Schenk, V., van der Straaten, F., & Mirmohammadi, M. (2009). Petrology, geochemistry, and geochronology of trondhjemites from the Qori Complex, Neyriz, Iran. *Lithos*, *112*, 413–433. https://doi.org/10.1016/j.lithos.2009.03.047

Fazlnia, N., Moradian, A., Rezaei, K., Moazen, M., & Alipour, S. (2007). Synchronous activity of anorthositic and S-type granitic magmas in Chah-Dozdan batholith, Neyriz, Iran: evidence of zircon SHRIMP and monazite CHIME dating. *Journal of Sciences, Islamic Republic of Iran*, *18*, 221–237.

Fürsich, F. T., Wilmsen, M., Seyed-Emami, K., & Majidifard, M. R. (2009). Lithostratigraphy of the upper Triassic-Middle Jurassic Shemshak group of northern Iran. *Geological Society Special Publication*, *312*, 129–160. https://doi.org/10.1144/SP312.6

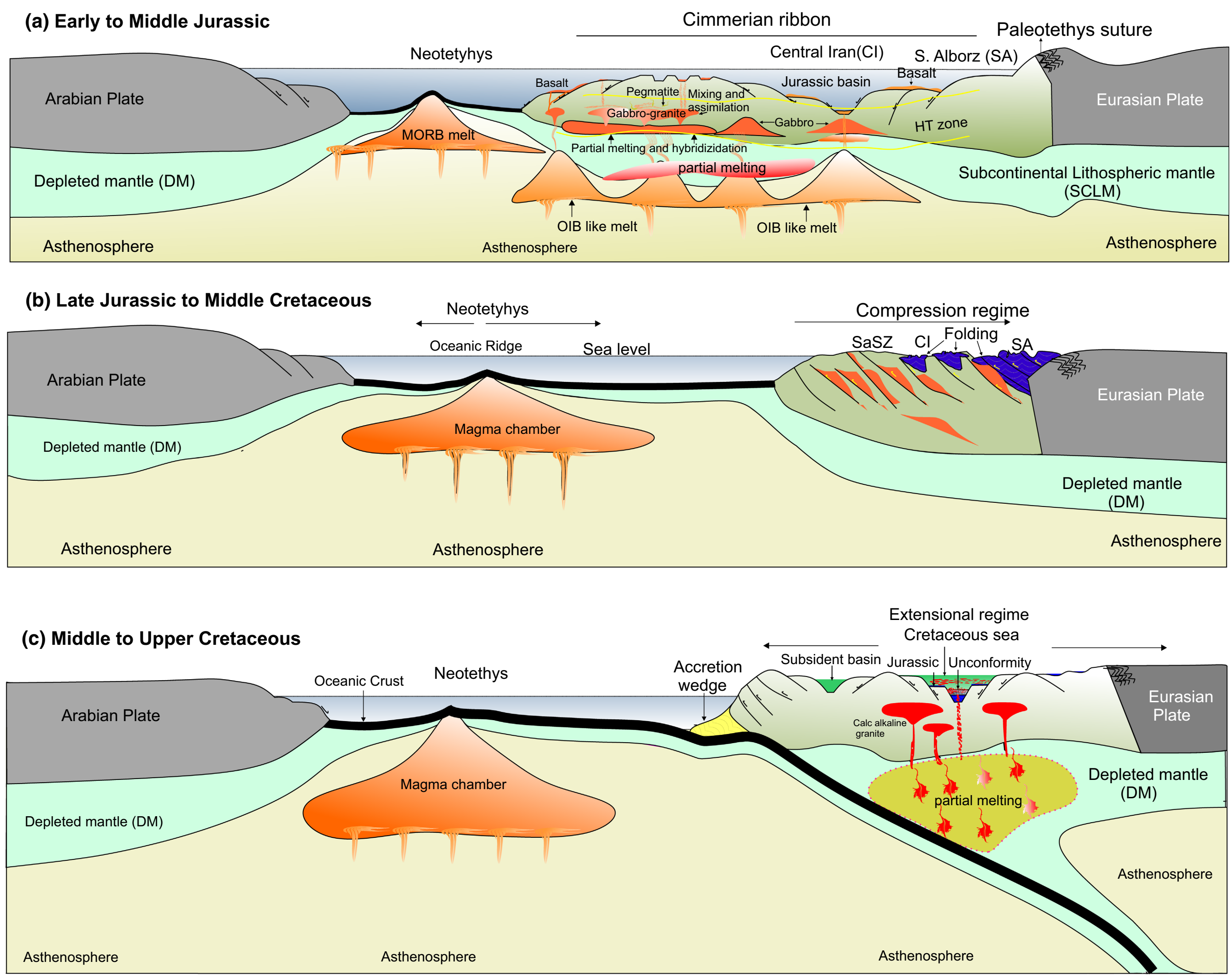

FIGURE 8 Schematic model for the Jurassic tectonic evolution of Turkey and Iran. (a) Development of Jurassic extensional basins in Iran and northern Turkey during Early–Middle Jurassic associated with bimodal magmatism. (b) Expansion of Neotethys into western Iran, with basin inversion and exposure in the Late Jurassic–Early Cretaceous. (c) Subduction of Neotethys and development of forearc, arc magmatism and back-arc basin magmatism. See the text for more explanation. [Colour figure can be viewed at wileyonlinelibrary.com]

Gallahue, M. M., Stein, S., Stein, C. A., Jurdy, D., Barklage, M., & Rooney, T. O. (2020). A compilation of igneous rock volumes at volcanic passive continental margins from interpreted seismic profiles. *Marine and Petroleum Geology*, *122*, 104635. https://doi.org/10.1016/J.MARPETGEO.2020.104635

Galoyan, G. L., Melkonyan, R. L., Atayan, L. S., Chung, S. L., Khorenyan, R. H., Lee, Y. H., & Amiraghyan, S. V. (2018). On the petrology and geochemistry of Jurassic magmatics of the Somkheti segment of Somkheto-Karabagh tectonic zone (Northern Armenia). *Proceedings of the NAS RA: Earth Sciences*, *71*, 3–227.

Genç, Ş. C., & Tüysüz, O. (2010). Tectonic setting of the Jurassic bimodal magmatism in the Sakarya Zone (Central and Western Pontides), Northern Turkey: A geochemical and isotopic approach. *Lithos*, *118*, 95–111. https://doi.org/10.1016/J.LITHOS.2010.03.017

Gholipour, S., Azizi, H., Masoudi, F., Asahara, Y., & Minami, M. (2022). S-type like granites and felsic volcanic rocks in the Mahabad area, NW Iran: Late Neoproterozoic extensional tectonics follow collision on the northern boundary of Gondwana. *Lithos*, *416–417*, 106658. https://doi.org/10.1016/J.LITHOS.2022.106658

Gholipour, S., Azizi, H., Masoudi, F., Asahara, Y., & Tsuboi, M. (2021). Zircon U-Pb ages, geochemistry, and Sr-Nd isotope ratios for early cretaceous magmatic rocks, southern Saqqez, northwestern Iran. *Geochemistry*, *81*, 125687. https://doi.org/10.1016/j.chemer.2020.125687

Günay, K., Dönmez, C., Oyan, V., Baran, C., Çiftçi, E., Parlak, O., Yıldırım, N., Deng, X. H., Li, C., Yıldırım, E., & Özkümüş, S. (2019). Geology, geochemistry and Re-Os geochronology of the Jurassic Zeybek volcanogenic massive sulfide deposit (Central Pontides, Turkey). *Ore Geology Reviews*, *111*, 102994. https://doi.org/10.1016/j.oregeorev.2019.102994

Hassanpour, S. (2021). Lahroud, a Paleo-Tethys Remnant in Northwestern Iran: Implications for Geochemistry, Radioisotope Geochronology, and Tectonic Setting. *Russian Geology and Geophysics*, *62*, 1107–1126. https://doi.org/10.2113/rgg20194116

Hunziker, D., Burg, J.-P., Bouilhol, P., & von Quadt, A. (2015). Jurassic rifting at the Eurasian Tethys margin: Geochemical and geochronological constraints from granitoids of North Makran, southeastern Iran. *Tectonics*, *34*, 571–593. https://doi.org/10.1002/2014TC003768

Irvine, T. N., & Baragar, W. R. A. (1971). A Guide to the chemical classification of the common volcanic rocks. *Canadian Journal of Earth Sciences*, *8*, 523–548. https://doi.org/10.1139/e71-055

Kandemir, R., & Yilmaz, C. (2009). Lithostratigraphy, facies, and deposition environment of the lower Jurassic Ammonitico Rosso type sediments (ARTS) in the Gümüşhane area, NE Turkey: Implications for the opening of the northern branch of the Neo-Tethys Ocean. *Journal of Asian Earth Sciences*, *34*, 586–598. https://doi.org/10.1016/J.jeaes.2008.08.006

Karimpour, M. H., Stern, C. R., & Farmer, G. L. (2010). Zircon U–Pb geochronology, Sr–Nd isotope analyses, and petrogenetic study of the Dehnow diorite and Kuhsangi granodiorite (Paleo-Tethys), NE Iran. *Journal of Asian Earth Sciences*, *37*, 384–393. https://doi.org/10.1016/j.jseaes.2009.11.001

Karsli, O., Dokuz, A., Faruk, U., & Bin, A. (2010). Relative contributions of crust and mantle to generation of Campanian high-K calc-alkaline I-type granitoids in a subduction setting, with special reference to the Harşit Pluton, Eastern Turkey. *Contributions to Mineralogy and Petrology*, *160*, 467–487. https://doi.org/10.1007/s00410-010-0489-z

Karsli, O., Dokuz, A., & Kandemir, R. (2017). Zircon Lu-Hf isotope systematics and U–Pb geochronology, whole-rock Sr-Nd isotopes and geochemistry of the Early Jurassic Gokcedere pluton, Sakarya Zone-NE Turkey: a magmatic response to roll-back of the Paleo-Tethyan oceanic lithosphere. *Contributions to Mineralogy and Petrology*, *172*, 31. https://doi.org/10.1007/s00410-017-1346-0

Karsli, O., Dokuz, A., Uysal, İ., Aydin, F., Kandemir, R., & Wijbrans, J. (2010). Generation of the Early Cenozoic adakitic volcanism by partial melting of mafic lower crust, Eastern Turkey: Implications for crustal thickening to delamination. *Lithos*, *114*, 109–120. https://doi.org/10.1016/j.lithos.2009.08.003

Karsli, O., Şengün, F., Santos, J. F., Uysal, İ., Dokuz, A., Aydin, F., & Kandemir, R. (2022). Late Jurassic Paleotethyan oceanic slab break-off revealed by Sr-Nd-Hf isotopes of Na-rich adakitic granites from northwestern Turkey. *Gondwana Research*, *103*, 205–220. https://doi.org/10.1016/J.GR.2021.11.014

Khalaji, A. A., Esmaeily, D., Valizadeh, M. V., & Rahimpour-Bonab, H. (2007). Petrology and geochemistry of the granitoid complex of Boroujerd, Sanandaj-Sirjan Zone, Western Iran. *Journal of Asian Earth Sciences*, *29*, 859–877. https://doi.org/10.1016/j.jseaes.2006.06.005

Le Bas, M., Maitre, R., Streckeisen, A., & Zanettin, B. (1986). A chemical classification of volcanic rocks based on the total alkali-silica diagram. *Journal of Petrology*, *27*, 745–750. https://doi.org/10.1093/petrology/27.3.745

Lechmann, A., Burg, J.-P. P., Ulmer, P., Mohammadi, A., Guillong, M., & Faridi, M. (2018). From Jurassic rifting to Cretaceous subduction in NW Iranian Azerbaijan: Geochronological and geochemical signals from granitoids. *Contributions to Mineralogy and Petrology*, *173*, 102. https://doi.org/10.1007/s00410-018-1532-8

MacLean, W. H. H., & Barrett, T. J. J. (1993). Lithogeochemical techniques using immobile elements. *Journal of Geochemical Exploration*, *48*, 109–133. https://doi.org/10.1016/0375-6742(93)90002-4

Madanipour, S., Ehlers, T. A., Yassaghi, A., & Enkelmann, E. S. (2015). Time-temperature U-Th-Pb-He modelling of the Lisar Granite in the Talesh Mountains, evidence for late cenozoic exhumation pattern at NW Iranian Plateau (in Persian). In *The first meeting of Tectonic and Structural Geology Association of Iran*.

Maffione, M., & van Hinsbergen, D. J. J. (2018). Reconstructing plate boundaries in the Jurassic Neo-Tethys from the East and West Vardar Ophiolites (Greece and Serbia). *Tectonics*, *37*, 858–887. https://doi.org/10.1002/2017TC004790

Mahmoudi, S., Corfu, F., Masoudi, F., Mehrabi, B., & Mohajjel, M. (2011). U-Pb dating and emplacement history of granitoid plutons in the northern Sanandaj-Sirjan Zone, Iran. *Journal of Asian Earth Sciences*, *41*, 238–249. https://doi.org/10.1016/j.jseaes.2011.03.006

Miyashiro, A. (1973). The Troodos ophiolitic complex was probably formed in an island arc. *Earth and Planetary Science Letters*, *19*, 218–224. https://doi.org/10.1016/0012-821X(73)90118-0

Miyashiro, A. (1974). Volcanic rock series in island arcs and active continental margins. *American Journal of Science*, *274*, 321–355. https://doi.org/10.2475/ajs.274.4.321

Moghadam, H. S., Li, Q. L., Griffin, W. L., Stern, R. J., Santos, J. F., Lucci, F., Beyarslan, M., Ghorbani, G., Ravankhah, A., Tilhac, R., & O'Reilly, S. Y. (2021). Prolonged magmatism and growth of the Iran-Anatolia Cadomian continental arc segment in Northern Gondwana. *Lithos*, *384–385*, 105940. https://doi.org/10.1016/J.Lithos.2020.105940

Moghadam, H. S., & Stern, R. J. (2021). Subduction initiation causes broad upper plate extension: The Late Cretaceous Iran example. *Lithos*, *398–399*, 106296. https://doi.org/10.1016/j.lithos.2021.106296

Mousivand, F., Rastad, E., Meffre, S., Peter, J. M., Solomon, M., & Zaw, K. (2011). U-Pb geochronology and Pb isotope characteristics of the Chahgaz volcanogenic massive sulphide deposit, southern Iran. *International Geology Review*, *53*, 1239–1262. https://doi.org/10.1080/00206811003783364

Mullen, E. D. (1983). MnO/TiO2/P2O5: a minor element discriminant for basaltic rocks of oceanic environments and its implications for petrogenesis. *Earth and Planetary Science Letters*, *62*, 53–62. https://doi.org/10.1016/0012-821X(83)90070-5

Nouri, F., Asahara, Y., Azizi, H., Yamamoto, K., & Tsuboi, M. (2017). Geochemistry and petrogensis of the Eocene back arc mafic rocks in the Zagros suture zone, northern Noorabad, western Iran. *Chemie der Erde - Geochemistry*, *77*, 517–533. https://doi.org/10.1016/j.chemer.2017.06.002

Nouri, F., Azizi, H., Asahara, Y., & Stern, R. J. R. J. (2021). A new perspective on Cenozoic calc-alkaline and shoshonitic volcanic rocks, eastern Saveh (central Iran). *International Geology Review*, *63*, 476–503. https://doi.org/10.1080/00206814.2020.1718005

Pearce, J. A. (2008). Geochemical fingerprinting of oceanic basalts with applications to ophiolite classification and the search for Archean oceanic crust. *Lithos*, *100*, 14–48. https://doi.org/10.1016/j.lithos.2007.06.016

Pearce, J. A. (2014). Immobile element fingerprinting of ophiolites. *Elements*, *10*, 101–108. https://doi.org/10.2113/gselements.10.2.101

Sarifakioğlu, E., Özen, H., & Winchester, J. A. (2009). Whole rock and mineral chemistry of ultramafic-mafic cumulates from the Orhaneli (Bursa) ophiolite, NW Anatolia. *Turkish Journal of Earth Sciences*, *18*, 55–83.

Şen, C. (2007). Jurassic Volcanism in the Eastern Pontides: Is it Rift related or Subduction related? *Turkish Journal of Earth Sciences*, *16*, 523–539.

Sengör, A. M. C., & Yilmaz, Y. (1981). Tethyan evolution of Turkey: A plate tectonic approach. *Tectonophysics*, *75*, 181–241. https://doi.org/10.1016/0040-1951(81)90275-4

Shahbazi, H., Siebel, W., Pourmoafee, M., Ghorbani, M., Sepahi, A. A., Shang, C. K., & Vousoughi Abedini, M. (2010). Geochemistry and U-Pb zircon geochronology of the Alvand plutonic complex in Sanandaj-Sirjan Zone (Iran): New evidence for Jurassic magmatism. *Journal of Asian Earth Sciences*, *39*, 668–683. https://doi.org/10.1016/j.jseaes.2010.04.014

Shakerardakani, F., Neubauer, F., Masoudi, F., Mehrabi, B., Liu, X., Dong, Y., Mohajjel, M., Monfaredi, B., & Friedl, G. (2015). Panafrican basement and Mesozoic gabbro in the Zagros orogenic belt in the Dorud–Azna region (NW Iran): Laser-ablation ICP–MS zircon ages and geochemistry. *Tectonophysics*, *647*, 146–171. https://doi.org/10.1016/j.tecto.2015.02.020

Shervais, J. W. (1982). Ti–V plots and the petrogenesis of modern and ophiolitic lavas. *Earth and Planetary Science Letters*, *59*, 101–118. https://doi.org/10.1016/0012-821X(82)90120-0

Stern, R. J., Moghadam, H. S., Pirouz, M., & Mooney, W. (2021). The geodynamic evolution of Iran. *Annual Review of Earth and Planetary Sciences*, *49*, 9–36. https://doi.org/10.1146/annurev-earth-071620-052109

Stöcklin, J., & Nabavi, M. H. (1973). *Tectonic Map of Iran, Scale 1:2500000*. Geological Survey of Iran.

Topuz, G., Altherr, R., Schwarz, W. H., Siebel, W., Satır, M., & Dokuz, A. (2005). Post-collisional plutonism with adakite-like signatures: The Eocene Saraycık granodiorite (Eastern Pontides, Turkey). *Contributions to Mineralogy and Petrology*, *150*, 441–455. https://doi.org/10.1007/s00410-005-0022-y

Topuz, G., Candan, O., Zack, T., & Yılmaz, A. (2017). East Anatolian plateau constructed over a continental basement: No evidence for the East Anatolian accretionary complex. *Geology*, *45*, 791–794. https://doi.org/10.1130/G39111.1

Topuz, G., Çelik, Ö. F., Şengör, A. M. C., Altintaş, I. E., Zack, T., Rolland, Y., & Barth, M. (2013). Jurassic ophiolite formation and emplacement as backstop to a subduction-accretion complex in northeast Turkey, the Refahiye ophiolite, and relation to the Balkan ophiolites. *American Journal of Science*, *313*, 1054–1087. https://doi.org/10.2475/10.2013.04

Topuz, G., Göçmengil, G., Rolland, Y., Çelik, Ö. F., Zack, T., & Schmitt, A. K. (2013). Jurassic accretionary complex and ophiolite from northeast Turkey: No evidence for the Cimmerian continental ribbon. *Geology*, *41*, 255–259. https://doi.org/10.1130/G33577.1

Uysal, I., Akmaz, R. M., Kapsiotis, A., Demir, Y., Saka, S., Avci, E., & Müller, D. (2015). Genesis and geodynamic significance of chromitites from the Orhaneli and Harmancık ophiolites (Bursa, NW Turkey) as evidenced by mineralogical and compositional data. *Ore Geology Reviews*, *65*, 26–41. https://doi.org/10.1016/J.OREGEOREV.2014.08.006

Uysal, I., Ersoy, E. Y., Dilek, Y., Escayola, M., Sarifakioğlu, E., Saka, S., & Hirata, T. (2015). Depletion and refertilization of the Tethyan oceanic upper mantle as revealed by the early Jurassic Refahiye ophiolite, NE Anatolia—Turkey. *Gondwana Research*, *72*, 594–611. https://doi.org/10.1016/j.gr.2013.09.008

Withjack, M., Malinconico, M., & Durcanin, M. (2020). The “Passive” margin of Eastern North America: Rifting and the influence of prerift orogenic activity on postrift development. *Lithosphere*, *2020*, 8876280.

Yilmaz, O., & Bonhomme, M. G. (1991). *K-Ar isotopic age evidence for a Lower to Middle Jurassic low-pressure and a Lower Cretaceous high-pressure metamorphic events in north-central, Turkey*. International symposium on the geology of the Black Sea region.

Yunliang, W., Chengjiang, Z., & Shuzhi, X. (2001). Th/Hf-Ta/Hf identification of tectonic setting of basalts. *Acta Petrologica Sinica*, *17*, 413–421.

Zanchi, A., Zanchetta, S., Berra, F., Mattei, M., Garzanti, E., Molyneux, S., Nawab, A., & Sabouri, J. (2009). The Eo-Cimmerian (Late? Triassic) orogeny in North Iran. *Geological Society Special Publication*, *312*, 31–55. https://doi.org/10.1144/SP312.3

Zhang, C. L., Zou, H. B., Yao, C. Y., & Dong, Y. G. (2014). Origin of Permian gabbroic intrusions in the southern margin of the Altai Orogenic belt: A possible link to the Permian Tarim mantle plume? *Lithos*, *204*, 112–124. https://doi.org/10.1016/j.lithos.2014.05.019

Zhang, H., Chen, J., & Yang, T. (2018). Jurassic granitoids in the northwestern Sanandaj–Sirjan Zone: Evolving magmatism in response to the development of a Neo-Tethyan slab window. *Gondwana Research*, *62*, 269–286. https://doi.org/10.1016/j.gr.2018.01.012

SUPPORTING INFORMATION

Additional supporting information can be found online in the Supporting Information section at the end of this article.

Table S1. Number and references in the Figure 1.

Table S2. Whole-rock chemistry of Early–Middle Jurassic rocks Iran and Turkey.

Table S3. The isotope ratios of Early–Middle Jurassic rocks

How to cite this article: Azizi, H., Stern, R. J., Kandemir, R., & Karsli, O. (2023). A Jurassic volcanic passive margin in Iran and Turkey. *Terra Nova*, *35*, 141–152. https://doi.org/10.1111/ter.12638